A Measurement Study of FMCW Radar Configurations for Non-contact Vital Signs Monitoring

Zongxing Xie*, Yindong Hua*, and Fan Ye Department of Electrical and Computer Engineering, Stony Brook University {zongxing.xie, yindong.hua, fan.ye}@stonybrook.edu

Abstract—Non-contact vital signs monitoring (NCVSM) with radio frequency (RF) is attracting increasing attention due to its non-invasive nature. Recent advances in COTS radar technologies accelerate the development of RF-based solutions. While researchers have implemented and demonstrated the feasibility of NCVSM with diverse radar hardware, most efforts have been focused on devising algorithms to extract vital signs, with limited understanding about the effects of radar configurations. The deficiency in such understanding hinders the design of softwaredefined radar (SDR) optimally customized for NCVSM. In this work, we first hypothesize the effects of FMCW radar configurations using signal-to-interference-plus-noise ratio (SINR) based signal modeling, then we conduct extensive experiments with a COTS FMCW radar, TinyRad, to understand how various parameters impact NCVSM performance compared to a medical device. We find that a larger bandwidth or higher transmitting power in general improves vital sign estimation accuracy; however, coherent processing of consecutive chirps (time diversity) or multiple receiving antennas (space diversity) does not improve the performance. Observations on the baseband (BB) signal show that coherent processing contributes to a higher amplitude but similar phase patterns, whose periodic changes are the key in extracting vital signs.

Index Terms—Radar Configurations, Non-contact vital signs monitoring, Frequency-Modulated Continuous Wave (FMCW)

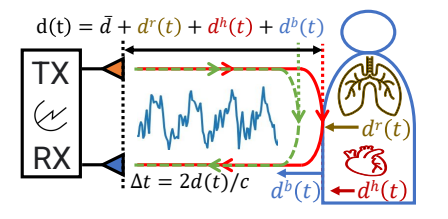
I. INTRODUCTION

Continuous monitoring of vital signs, such as respiration rate (RR) and heart rate (HR), is critical to health status assessment in either detecting changes in an individual's health (e.g., onset of flu or COVID) or tracking the progression in chronic diseases.

Conventional vital signs measurement solutions using Electrocardiogram (ECG) and photoplethysmography (PPG) have been made available on mobile devices and wearables (e.g., Apple watch, Fitbit). However, charging and wearing them regularly pose significant physical and cognitive user burdens, especially among older people. Thus adherence over long time for continuous monitoring is frequently difficult. Non-contact methods using cameras, acoustics, and RF avoid such burdens. RF methods are most promising because they are not impacted by environmental factors (e.g., lighting, noises), and do not produce visual images that cause privacy concerns.

The human body movement in the RF environment alters the scattered signal in the energy and travel distance. In particular,

This work is supported in part by NSF grants 1951880, 2028952, 2119299. * Co-primary authors.



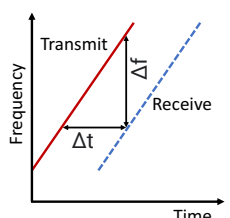


Fig. 1: The chest wall displacement due to respiration, heartbeat movements and body movement changes the time of flight (ToF) Δt thus phase of the scattered signal periodically, which allows vital signs extractions.

Fig. 2: FMCW measures range based on the linear relationship between ToF Δt of RX signal and its frequency shift Δf compared to TX signal.

the chest wall displacements due to respiration and heartbeat movements modulate the scattered signal with periodic changes in the phase, from which vital signs can be extracted (as illustrated in Fig. 1). Researchers have demonstrated the feasibility of NCVSM using radar techniques on commoditygrade hardware (e.g., FMCW) that strikes a balance between cost and performance [1, 2].

However, there has been a lack of systematic understanding of how different radar parameters (e.g., the bandwidth, chirp duration, chirp repetition interval, TX power, time/space diversity gains) impact the performance of NCVSM. Despite a plethora of work [3–7], most focused on the algorithms for vital sign extraction on different hardware, with some [2] comparing architectures between IR-UWB and FMCW.

In this work, we study how different radar parameters impact NCVSM performance. Our primary performance metric is the vital signs estimation error, defined as the difference between radar estimated vital sign values and the ground truth from a medical grade device. We explore questions including: How do the waveform parameters (e.g., bandwidth, up-chirp duration, chirp repetition interval) impact NCVSM? Does increasing TX power improve accuracy? How does coherent processing gain from time/space diversity (at RX) relate to the accuracy? Such knowledge and insights will offer directions in the design of future software-defined radars (SDR) customized for NCVSM.

To tackle the above questions, we leverage the flexibility of EV-Tinyrad24G (TinyRad for simplicity) from Analog Devices [8], a COTS FMCW radar evaluation board, with a set of reconfigurable parameters. FMCW achieves ranging

discrimination based on the linear relationship (as illustrated in Fig. 2) between the frequency shift and the time of flight (ToF), from which the targets can be distinguished from clutters at different distances [9]. We also provide qualitative analysis on the baseband (BB) signal to explain the impact of different radar configurations.

We summarize the contributions of this measurement study:

- We provide signal modeling to help understand the effects of different radar parameters in NCVSM. Based on that, we hypothesize how the changes in radar parameters may impact the BB signal and end-to-end (e2e) performance, and then design a set of experiments to verify those hypotheses accordingly.
- We conduct extensive real-life experiments for about 35 hours with 4 human subjects, collecting NCVSM data to examine the effects of a set of radar configurations (e.g., bandwidth, up-chirp duration, chirp repetition interval, TX power, diversity gain) with a COTS FMCW radar.
- We use the e2e NCVSM accuracy compared to a medical device to analyze the effects of radar configurations. We inspect the BB signal in the IQ plane to provide both temporal and spectral analysis, which allows us to attribute the e2e effects to corresponding causes. We find that the bandwidth is the most effective factor to improve NCVSM accuracy in cluttered environments, while surprisingly the space diversity gain with digital beamforming (DBF) and time diversity gain with multiple chirps in coherent processing interval (CPI) only amplify the amplitude of the BB signal but present similar phase patterns, thus ineffective for the NCVSM accuracy.

The contribution of this work lies in a fundamental understanding and insights on how different radar parameters impact the performance of NCVSM. Such insights pave the way to optimize software defined radar design for NCVSM.

II. PRELIMINARIES

In this section, we focus on modeling radar signals for NCVSM as a theoretical foundation, then hypothesize how different radar parameters impact the signal model.

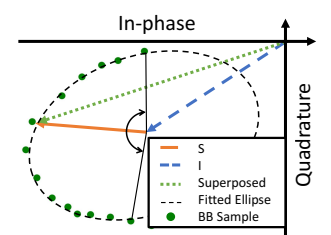
A. Modeling Radar Signal for NCVSM

In an ideal case of NCVSM, the received signal can be expressed as:

$$s(\tau, t) = p(\tau) * h(\tau, t) + n(\tau, t)$$

= $\alpha_d p(\tau - \tau_d(t)) + \sum_{i=1}^{n} \alpha_i p(\tau - \tau_i) + n(\tau, t),$ (1)

where p is the transmitted waveform (e.g., IR-UWB and FMCW) adopted by radars; τ is a small-scale (fast) time measurement to describe the ToF of the scattered RF signal; t is in a larger (slow) time scale along which the channel impulse response (CIR) h at a certain distance is changing (e.g., due to the human body movement). n denotes the random noise. α denotes magnitudes of CIR due to the target d and the static objects i; the two-way echo delay $\tau_d(t) = 2d(t)/c$ indicates the distance of the chest wall from



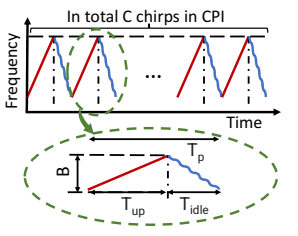


Fig. 3: During the chest wall displacement, the received BB samples move back and forth periodically along an elliptical arc in the IQ plane, allowing vital signs extraction.

Fig. 4: A set of parameters related to the FMCW waveform are re-configurable, and their effects on NCVSM will be examined.

the radar: $d(t) = \bar{d} + d^{\rm r}(t) + d^{\rm h}(t) + d^{\rm b}(t)$, where \bar{d} is the nominal distance between the chest wall and the radar, and the rest three terms are displacements due to respiration, heartbeat and body movement. When the RF signal scattered from the human body is separable from the clutter with the radar range resolution, the BB signal can be modeled as:

$$y(t) = \alpha_d e^{-j2d(t)\kappa} + \omega, \tag{2}$$

where $\kappa=2\pi/\lambda$ denotes the angular wavenumber determined by the wavelength λ , and ω denotes a negligible complex number as random noise. Thus, the chest wall displacement due to respiration and heartbeat can be easily extracted from the phase in (2) when the person stays stationary.

However, in the real case, the received signal is more complex than the reflection from a point scatterer. Instead, it is a superposition of the interference from the clutter (including multipath) and the signal scattered from the human body, which has a 3D shape and should be modeled as a collection of point scatterers at different depths, and they will interfere with each other constructively or destructively. If we group the scattered signals into the set of moving part (denoted by M) and the set of static part including clutter (denoted by N) respectively, it can be expressed as: 1

$$y(t) = \sum_{m \in M} \alpha_m e^{-j(\phi_m + 2d(t)\kappa)} + \sum_{n \in N} \alpha_n e^{-j(\phi_n + 2\bar{d}\kappa)}$$

$$= \alpha_{\bar{m}} e^{-j\phi_{\bar{m}}} e^{-j2d(t)\kappa} + \alpha_{\bar{n}} e^{-j\phi_{\bar{n}}} e^{-j2\bar{d}\kappa}$$

$$= S + I,$$
(3)

where the subscripts m and n denote the elements from the set M and set N separately, \bar{m} and \bar{n} denote the resulting terms of their respective superposition, and ϕ denotes the phase offset due to the relative distance between point scatterers. S denotes the interesting signal of the moving part, which is modulated by the chest wall displacement thus periodic phase changes from vital signals; I denotes the signal scattered from the static part and clutter, as an interference to the interesting signal. As illustrated in Fig. 3, the trajectory of the received BB signal in IQ plane is moving back and forth along an arc (the effect of S), whose center is an offset (the effect of I) from the origin point due to interference from the static part.

 1 We assume that all scatterers in the set M follow the same movement pattern with different distances thus phases, and ignore the random noise.

B. Roles of Configurable Radar Parameters in Signal Model

Based on the above modeling, the received signal is the superposition of the interesting part S and the interference part I plus random noise ω . However, while S is the only part modulated with vital signals, we can only use the superposed signal to extract vital signs as it is not directly separable. So we believe the ratio of the received energy (denoted by E) between these components is critical to the e2e performance of NCVSM. Such ratio can be expressed as signal-to-interference-plus-noise ratio (SINR= $\frac{E_S}{E_I+E_{\omega}}$). 2

We will make some conjectures about how each reconfigurable radar parameter may impact NCVSM from the perspective of SINR based on the radar principles as follows:

Bandwidth (B) will determine the range resolution expressed as $\delta r = \frac{c}{2B}$ according to time-frequency duality. With a larger bandwidth, a finer grained range resolution may suffer less interference from scatterers in clutter, thus better SINR, which may improve the accuracy of NCVSM.

Up-chirp duration (T_{up}) will determine the energy of the TX signal in a linear relationship expressed as $E_t = P_t \cdot T_{up}$. However, a longer T_{up} may increase both the energy of interesting signal and interference. It is not immediately clear how it may impact NCVSM performance.

Chirp repetition interval (T_p) will determine how frequently the movement will be sampled in frames per second fps=1/ $(C\cdot T_p)$ as illustrated in Fig. 4. While changing T_p with longer idle time seems not to affect SINR, it may break the vital signs estimation when fps goes below the Nyquist Frequency of vital signals. We want to find where is the critical limit of T_p for NCVSM.

TX power (P_t) will determine how much human body will be illuminated, which is critical to SINR. We want to see how P_t may impact NCVSM.

In addition to the above parameters, coherent processing with a **number** (K **out of** C) **of chirps** in CPI or a **number** (L) **of array elements** will contribute to the RX gain. The coherent processing with K chirps or L array elements can be expressed as:

$$z(t) = \sum_{s=0}^{S-1} e^{-js\phi_0} y_s(t), \tag{4}$$

where S is the number of elements (i.e., K chirps or L array elements); z is the resulting signal after coherent processing; ϕ_0 is the phase shift due to difference in ToF between the received signal y_s of consecutive elements.

Increasing the gain can suppress the random noise, commonly used to improve radar performance. We conjecture such coherent processing gains may help improve NCVSM performance as well.

 2 The received energy of either interesting signal or interference can be expressed in a classic radar equation as: $E=P_r\times T=\frac{P_tG^2\sigma\lambda^2}{(4\pi)^3d^4}\times T,$ where P_r is RX power; T is the signal duration; P_t is TX power, G is the antenna gain, proportional to the antenna aperture; σ is the radar cross section (RCS) of the scatterer (either interesting part or interfering part); d is the nominal distance between the radar and the scatterer.

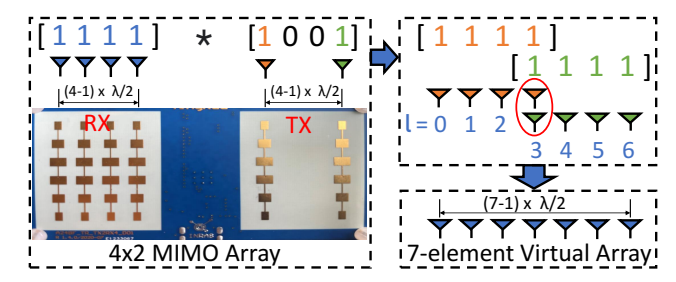


Fig. 5: The MIMO scheme has 2 TX and 4 RX. By switching between 2 TX to achieve orthogonality, the placement vector of the virtual array can be expressed as the convolution of the placement vectors of TX and RX arrays. The two elements (red circled) overlap to allow phase calibration between the two arrays (in orange and green) for the integrated 7-element virtual array.

<u>Remark.</u> While we make conjectures about the effects of each radar configurations from the perspective of SINR modeling, they remain informed guesses. We will use end-to-end experimental analysis to see whether such conjectures are indeed correct; and if not, what are the reasons behind. Such insights are the main goals in our experimental study.

III. EXPERIMENTAL SETUP AND METHODOLOGY

A. Experimental Setup

In this measurement study, we use a COTS FMCW radar, TinyRad, operating at a carrier frequency of 24 GHz. It has a MIMO scheme, with 4 RX and 2 TX as shown in Fig. 5, which can be integrated into a 7-element virtual array for the best space diversity.

To focus on the effects of varying radar configurations and eliminate impacts from the algorithm, we keep the algorithm the same for all the settings using a phase-based vital signs estimation pipeline proposed and implemented in [10, 11], which processes the signal in a 30-s sliding window. We use an FDA approved medical device, Masimo Pulse Oximeter [12], for the ground truth of RR and HR to evaluate the NCVSM.

B. Methodology

We first quantitatively examine the end-to-end performance of NCVSM with different radar configurations. Next, we inspect the received BB signal in IQ plane and the corresponding vital signals in both time and frequency domains to qualitatively analyze the changes in the signal patterns under different configurations.

We select a set of values for each parameter as shown in Table I for TinyRad. In experiments, when we vary the value of a certain parameter, we keep others unchanged using the default ones. We also study the effect of diversity gain by selecting different numbers of chirps (K out of C) and numbers of array elements (L) for coherent processing respectively. The settings of coherent processing gain will be described in $\S IV$ separately.

TABLE I: Parameter Settings

				-		
Parameter	Default	Configurable Values				
B (Mhz)	250	50	100	150	200	250
$T_{up} (\mu s)$	256	32	64	128	256	384
$T_p (\mu s)$	425	300	425	550	675	800
$P_t (dBm)$	8	-20	-13	-6	1	8

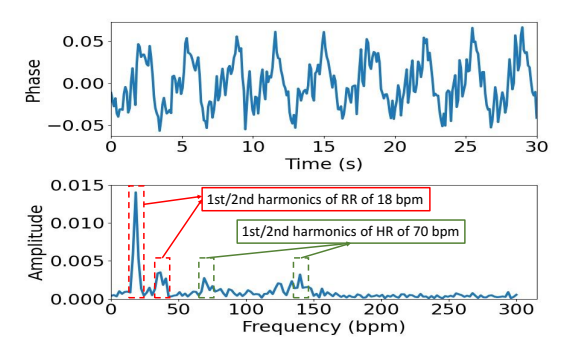


Fig. 6: In an example of a 30s window, the vital signal is modulated in the phase of RF signal. The periodicity of RR/HR in the time domain (top) yields condensed peaks in the frequency domain (bottom).

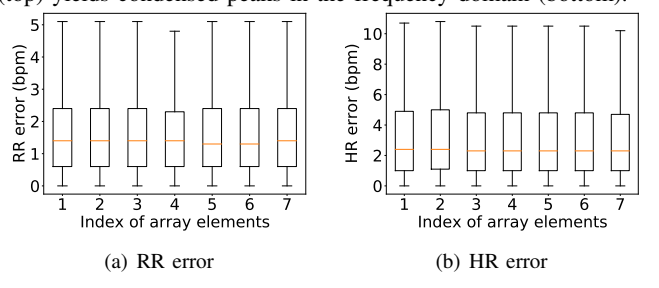


Fig. 7: The difference in vital signs error is negligible, with similar medians and distributions, between different array elements.

To mitigate the randomness from environmental variations and the inadvertent body motion, we conduct repeated experiments for data collection. For each aforementioned setting, we invite 4 volunteers to repeat the experiments 5 times with each session at 10 minutes, during which they are advised to stay stationary.

IV. EXPERIMENTS

In this section we show the results of experiments to examine the conjectures in §II-B with different radar configurations. Before diving into those experiments, we conduct a preliminary experiment using the default radar configuration to show that the difference between array elements in NCVSM errors with respect to the ground truth is negligible in Fig. 7. It is mainly because they are close to each other, thus their signals differ just by fixed phase offsets determined by antenna layout geometry. Therefore, we use data from all 7 array elements of repeated experiments by all volunteers to show the distribution of NCVSM accuracy in subsequent box-plots.

A. Bandwidth (B)

We first examine the effect of varying B on the performance of NCVSM as shown in Fig. 8. In addition to e2e performance, we also look at the extracted vital signal in each sliding window, and describe the patterns in the signal level by introducing a metric called the periodicity-to-noise ratio (PNR $_{r/h}$ for RR/HR respectively). ³ A large PNR indicates the periodicity of vital signal is strong in the time domain and

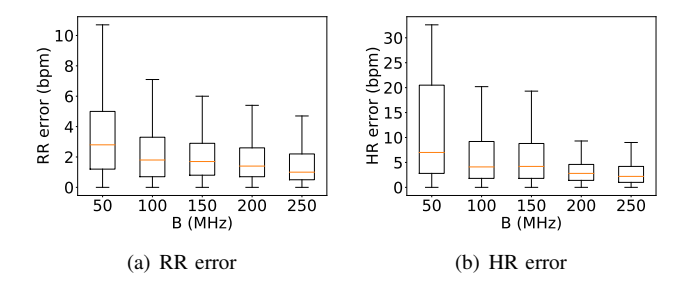


Fig. 8: As the bandwidth increases (50–250 MHz), the median error of RR/HR monotonically decreases from 3/7 bpm to 1/2.5 bpm.

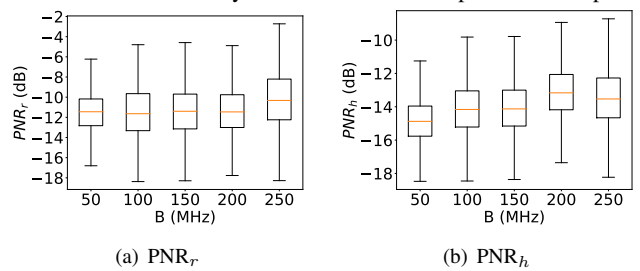


Fig. 9: $PNR_{r/h}$ show an upward trend with the increasing B, however it is not monotonic.

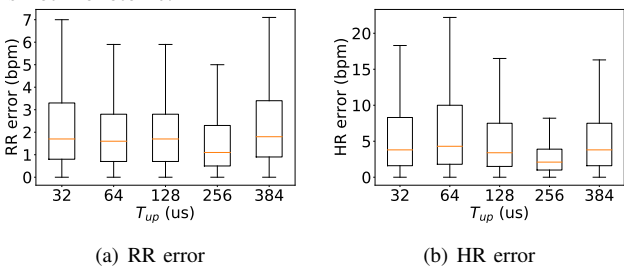


Fig. 10: The difference in RR/HR error between T_{up} (32–384 μs) is limited and mostly from randomness.

can be easily detected in the frequency domain as illustrated in Fig. 6. Fig. 9 shows the vital signs error and $PNR_{r/h}$ for different bandwidths. With an increasing B (50–250 MHz), we observe a downward trend in the vital signs error (with the median RR/HR error from 3/7 to 1/2.5 bpm) and an upward trend in $PNR_{r/h}$. Based on the results, we believe an increased B can improve $PNR_{r/h}$ and e2e accuracy by reducing the interference from clutter. This confirms our earlier conjecture. Note that $PNR_{r/h}$ itself has some slight fluctuations and is not directly related to the e2e performance.

B. Up-chirp Duration (T_{up})

Fig. 10 shows e2e performance with increasing T_{up} (32–384 μs). The trend is not monotonically increasing or decreasing in both RR/HR error. The variation in performance is however very limited, thus the impact of T_{up} is not obvious. We believe such variation is from randomness (e.g., inadvertent movement during data collection), albeit reasonably limited.

C. Chirp Repetition Interval (T_n)

We observe limited variations in e2e performance with the increasing T_p (300–800 μs) as shown in Fig. 11, except for an increased error in HR at $T_p=800$. As a longer T_p means a slower sampling rate, the sampling rate becomes

 $^{^{3}}$ PNR $_{r/h}$ is defined as the ratio of the summed power of the 1st/2nd harmonics of RR/HR to the rest spectrum, as both harmonics are used in the vital signs estimation pipeline.

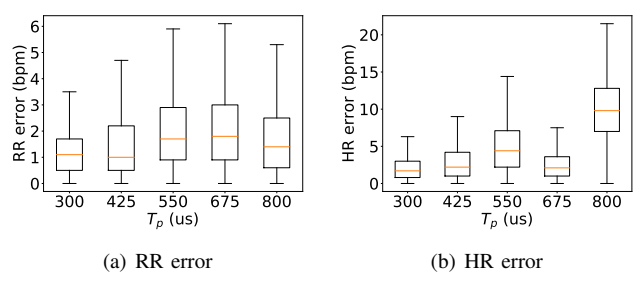


Fig. 11: As T_p increases, the variation in RR/HR error is limited except that when T_p reaches 800 μs , the sampling rate becomes slower than necessary for valid HR estimation algorithm.

only 5Hz when $T_p=800$. This becomes lower than the Nyquist frequency for sampling the second harmonic of HR, which is necessary for a valid HR estimation in our adopted signal processing pipeline. Based on the results, we believe the varying T_p will not impact NCVSM accuracy significantly, as long as the resulting sampling frequency is higher than the lower limit. Notably, the maximum unambiguous range of the radar is determined by T_p , which is now also confined by the necessary frequency of vital signs estimation algorithm. Therefore, the lower bound of T_p is set by the desired sensing range, while its upper bound is set by the necessary frequency for valid HR estimation. Such dual constraints needs careful consideration in future customized SDR.

D. TX power (P_t)

Fig. 12 shows NCVSM performance with increasing P_t (-20–8 dBm). While the variation in e2e RR error is limited (because respiration movements have much larger displacements thus stronger energy), it is interesting to see the HR error decreases with higher P_t . The difference in the trend between RR and HR may be attributed to the fact that the displacement and the scatterer associated to heartbeat is much smaller, thus higher TX power creates stronger HR signals. This is consistent with our earlier conjecture.

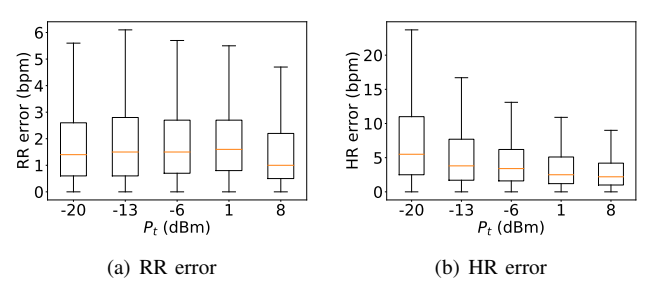


Fig. 12: While RR error is not sensitive to the increasing TX power, HR error shows a monotonic decrease (with median error 6–2.5 bpm).

E. Coherent Processing Gain with Time Diversity (K)

In this experiment, we pick BB signal from K (1–5) consecutive chirps out of a total C in CPI for coherent processing according to (4), while the phase shift between them can be considered negligible because the interval between chirps (i.e., $K \cdot T_p$) is much (about 100 times) shorter than a cycle of the vital signal (e.g., 1 s for the heartbeat of 60 bpm). The

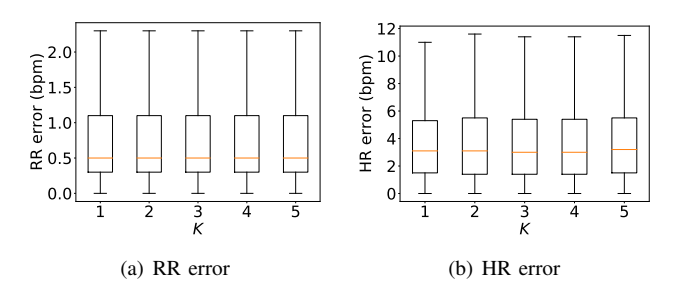


Fig. 13: While the gain increases with more (K from 1 to 5) chirps to be combined, the variation in RR/HR error is negligible.

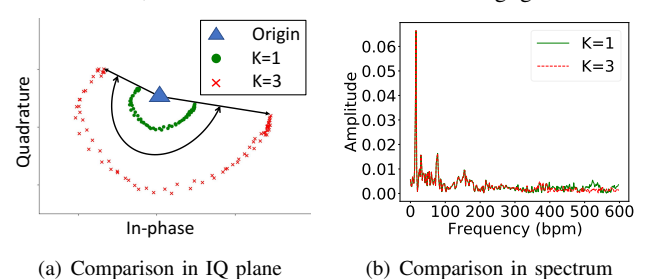


Fig. 14: An example of comparing between using 1 chirp and 3 chirps. Coherent processing only amplifies the radius of the elliptical arcs, but (a) neither alters the shape of the corresponding trajectory, (b) nor differs in the low frequency spectrum (0–300 bpm) used for vital signs extraction.

results with varying K in Fig. 13 shows that such coherent processing gain with time diversity does not improve NCVSM. This surprising discovery prompts us to further inspect the BB signal in the IQ plane. We note that the only difference between using different numbers of chirps is in the amplified radii of their elliptical trajectories. However, the relative angles of trajectories and their respective spectrum are almost the same (as illustrated by an example in Fig. 14). Thus the degree of phase periodicity remains similar. This explains the counterintuitive observation of the ineffectiveness of such coherent processing.

F. Coherent Processing Gain with Space Diversity (L)

Similarly, we combine the received signal at different array elements based on (4) with phase shift due to the angle of arrival (AoA). However, no improvement in NCVSM performance has been observed in Fig.15 with increasing L (at most 7) array elements for coherent processing. We show with an example that the extracted vital signal (i.e., relative phase change shown in Fig. 16(b)) is almost the same between using only 1 array element and using 3 array elements, except for an amplified amplitude in IQ plane as shown in Fig. 16(a). This explains again the counter-intuitive result. While the space diversity from MIMO has no direct contribution to NCVSM accuracy, it enables spatial filtering which potentially allows simultaneous monitoring of multiple users at different AoAs.

V. DISCUSSION

In this study, we extract vital signs using the phase of the received baseband signal, which is a superposition of the interesting signal and interference. The experimental results of the end-to-end evaluation inevitably have large errors from

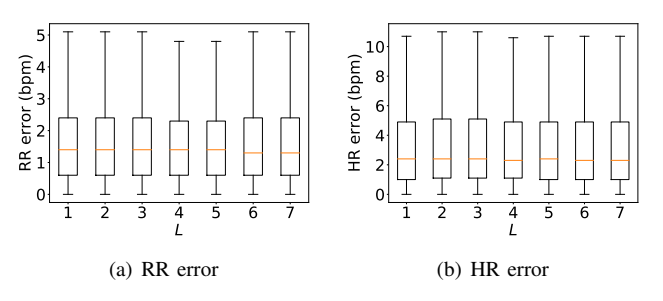


Fig. 15: Vital signs error remains mostly the same with increasing L array elements. Coherent processing gain is not improving accuracy.

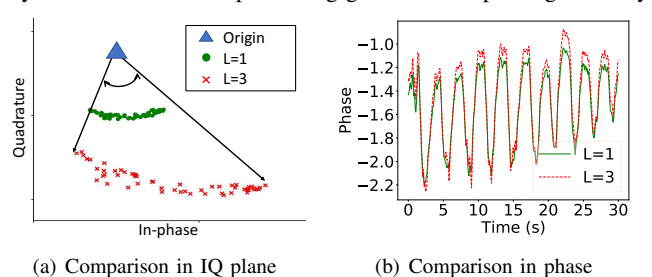


Fig. 16: An example of comparing between using 1 array element and 3 array elements. While combining 3 array elements amplifies (a) the radius of the elliptical arc, (b) the resulting phase is mostly the same as using 1 array element except for a negligible phase shift.

randomness during data collection, because of factors such as random body motion which cannot be eliminated. Nevertheless, we are still able to observe the statistical impact of radar parameters on the performance. To validate the effects of radar configurations with direct measure of respective signal components according to its model, we will investigate the algorithms for separating the interference component from the interesting signal in the future work, and we believe the estimation of the center of the elliptical arc is a critical step. In addition to the interference from static/clutter, inadvertent motion remains an open challenge as the interference to vital signals, while the heartbeat signal also suffers interference from respiration which is much stronger in both RCS and displacement. We will explore these challenges of NCVSM from the perspective of the scattering model; meanwhile, we will have larger subject pools to mitigate the randomness with sufficient diversity. From this study, we learn that the bandwidth is effective on the e2e performance of NCVSM by excluding clutter with range resolution. Due to space limit, we only focus on FMCW in this paper. The phase of the BB signal, as modeled in (2) for vital signs extraction, however, is independent of the waveform design (e.g., CW, stepped frequency CW, FMCW and IR-UWB). Thus we believe the understanding of radar configurations in this study is transferable to RF platforms with different waveform designs, which will be further investigated in the future work.

VI. RELATED WORK

Radar-based NCVSM has attracted researchers' attention for a few decades [13]. Most of the existing work focused on the algorithm design of vital signs extraction [3–7, 11], whereas many different configurations of radar parameters

have been studied for NCVSM. Empirical comparison between two popular radar architectures, IR-UWB and FMCW, was described in [2]. While they differ in the radar implementation, the effect of radar configurations on NCVSM works the same for both IR-UWB and FMCW in principle. Although both can be made fully re-configurable in principle, commercial off-the-shelf FMCW radars tend to offer more flexibility than IR-UWB ones [1, 5]. Researchers have also applied digital beamforming to achieve diversity gain and spatial filtering based on the MIMO scheme [4, 7]. However, the existing work lack a comprehensive discussion about the effects of radar configurations on NCVSM. We leverage the flexibility of a COTS FMCW radar to systematically compare the effects of radar configurations by performing extensive experiments with all re-configurable parameters such as bandwidth, up-chirp duration, chirp repetition interval, and TX power. Moreover, we explore the effects of both time and space diversity gain on NCVSM.

VII. CONCLUSION

In this paper, we study the effects of FMCW radar configurations on the non-contact vital signs monitoring. We carefully model the radar signal for vital signs extraction. Based on the signal modeling, we form hypotheses and design a set of experiments to collect observations accordingly. The experimental results show that the increased bandwidth can effectively help improve NCVSM accuracy as it reduce the interference from the clutter. However, the coherent processing gain at RX side does not improve NCVSM accuracy. We believe the observations we collected provide new understandings about radar-based NCVSM and suggest future directions for sensing-oriented SDR design with optimal trade-offs.

REFERENCES

- [1] A. Ahmad, J. C. Roh, D. Wang, and A. Dubey, "Vital signs monitoring of multiple people using a fmcw millimeter-wave sensor," in *IEEE RadarConf18*.
- [2] E. Antide, M. Zarudniev, O. Michel, and M. Pelissier, "Comparative study of radar architectures for human vital signs measurement," in *IEEE RadarConf20*.
- [3] N. Shimomura, M. Otsu, and A. Kajiwara, "Empirical study of remote respiration monitoring sensor using wideband system," in *IEEE ICSPCS*, 2012.
- [4] M. Mercuri, G. Sacco, R. Hornung, P. Zhang, H. Visser, M. Hijdra, Y.-H. Liu, S. Pisa, B. van Liempd, and T. Torfs, "2-d localization, angular separation and vital signs monitoring using a siso fmcw radar for smart long-term health monitoring environments," *IEEE 10T-J.* 2021.
- [5] S. M. Islam, N. Motoyama, S. Pacheco, and V. M. Lubecke, "Non-contact vital signs monitoring for multiple subjects using a millimeter wave fmcw automotive radar," in *IEEE/MTT-S IMS*, 2020, pp. 783–786.
- [6] M.-C. Huang, J. J. Liu, W. Xu, C. Gu, C. Li, and M. Sarrafzadeh, "A self-calibrating radar sensor system for measuring vital signs," *IEEE TBioCAS*, 2015.
- [7] J. Hinz and U. Zölzer, "A mimo fmcw radar approach to hfswr," Advances in Radio Science, vol. 9, no. C. 4-2, pp. 159–163, 2011.
- [8] Tinyrad. [Online]. Available: https://www.analog.com/en/design-center/ evaluation-hardware-and-software/evaluation-boards-kits/eval-tinyrad
- [9] A. G. Stove, "Linear fmcw radar techniques," in *IEE Proceedings F-Radar and Signal Processing*, vol. 139, no. 5. IET, 1992, pp. 343–350.
- [10] Z. Xie, B. Zhou, X. Cheng, E. Schoenfeld, and F. Ye, "Vitalhub: Robust, non-touch multi-user vital signs monitoring using depth camera-aided uwb," in 2021 IEEE 9th International Conference on Healthcare Informatics (ICHI). IEEE, 2021, pp. 320–329.
- [11] Z. Xie, B. Zhou, and F. Ye, "Signal quality detection towards practical non-touch vital sign monitoring," in *Proceedings of the 12th ACM Conference on Bioinformatics, Computational Biology, and Health Informatics*, 2021, pp. 1–9.
- [12] Masimo. [Online]. Available: https://www.masimo.com/mightysat
- [13] J. C. Lin, "Noninvasive microwave measurement of respiration," *Proceedings of the IEEE*, vol. 63, no. 10, pp. 1530–1530, 1975.